Invited paper *4th International Conference on Solid State Crystals*

OPTO-ELECTRONICS REVIEW **12**(4), 347–352

Quantitative mobility spectrum analysis (QMSA) in multi-layer semiconductor structures

J. ANTOSZEWSKI* and L. FARAONE

School of Electrical, Electronic and Computer Engineering, The University of Western Australia
35 Stirling Highway, Crawley WA 6009, Australia

For modern semiconductor heterostructures containing multiple populations of distinct carrier species, conventional Hall and resistivity data acquired at a single magnetic field provide far less information than measurements as a function of magnetic field. However, the extraction of reliable and accurate carrier densities and mobilities from the field-dependent data can present a number of difficult challenges, which were never fully overcome by earlier methods such as the multi-carrier fit, the mobility spectrum analysis of Beck and Anderson, and the hybrid mixed-conduction analysis. More recently, in order to overcome the limitations of those methods, several research groups have contributed to development of the quantitative mobility spectrum analysis (QMSA), which is now available as a commercial product. The algorithm is analogous to a fast Fourier transform, in that it transforms from the magnetic field B domain to the mobility μ domain. QMSA converts the field-dependent Hall and resistivity data into a visually-meaningful transformed output, comprising the conductivity density of electrons and holes in the mobility domain. In this article, we apply QMSA to both synthetic and real experimental data that are representative of modern semiconductor structures.

Keywords: resistivity, Hall effect, carrier mobility, carrier density, Fourier transform.

1. Introduction

Modern multilayer semiconductor structures usually contain multiple populations of distinct carrier species; thus, in order to characterise their transport properties, a more sophisticated analysis procedure than the classic Hall measurement at a single magnetic field is required. Such procedures have traditionally consisted of a multi-carrier fit (MCF) to the magnetic field dependent Hall data which, however, is not unique since the starting parameters such as number and type of carriers, and corresponding mobilities and densities need to be assumed [1,2]. In order to overcome this difficulty Beck and Anderson developed the mobility spectrum (MS) algorithm which numerically transforms the experimental magnetic field dependent Hall data into an easily interpreted plot of the dependence of the conductivity density function on mobility [3], in which each carrier contributing to the total conductivity appears as a separate peak at a given mobility. However, the condition for MS uniqueness is that its solution is the envelope rather than the true mobility spectrum and, as such, is inaccurate. Subsequently, Meyer *et al.* [4] proposed a hybrid approach in which the qualitative information contained in the MS is used to obtain starting parameters for the more accurate MCF procedure, albeit requiring a discrete value for each carrier mobility rather than allowing for a distribution of mobilities as proposed in the original MS technique [3]. An iterative approach to obtaining a numerically accurate MS was proposed by Dziuba and Gorska [5]. However, the shortcoming of this procedure is the inherent instability during the convergence process, which creates false peaks and oscillations in the final spectrum.

Based on previous attempts to obtain an accurate MS, an approach described by Antoszewski *et al.* [6], and known as quantitative mobility spectrum analysis (QMSA), has been developed and then systematically tested and improved [7–14]. By using the MS of Beck and Anderson as an initial function for a modified iterative procedure the inherent instability of previous iterative procedures is removed and a good fit to the experimental data is obtained. In this paper, we present and discuss the performance of QMSA for evaluating multilayer semiconductor structures.

2. Multi-carrier systems

For a Hall sample involving more than one type of carrier, the longitudinal and transverse conductivity tensor components σ_{xx} and σ_{xy}, respectively, can be expressed as a sum over the m species present within the multi-carrier system [3]

$$\begin{aligned}\sigma_{xx}(B) &= \frac{1}{\rho(B)\{[R_H(B)B/\rho(B)]^2+1\}} = \sum_{i=1}^{m}\frac{en_i\mu_i}{1+(\mu_i B)} \\ \sigma_{xy}(B) &= \frac{R_H(B)B/\rho(B)}{\rho(B)\{[R_H(B)B/\rho(B)]^2+1\}} = \sum_{i=1}^{m} S_i\frac{en_i\mu_i^2 B}{1+(\mu_i B)^2}\end{aligned}, \quad (1)$$

*e-mail: jarek@ee.uwa.edu.au

where B is the applied magnetic field in the z direction, $R_H(B)$ and $\rho(B)$ are the experimental magnetic field dependent Hall coefficient and resistivity, respectively, n_i and μ_i are the concentration and mobility of the i^{th} carrier species, respectively, and S_i is +1 for holes and –1 for electrons. It is primarily the $(1 + \mu^2B^2)$ terms in the denominators of Eq. (1) which separate the contributions from the various carrier species. Note that the above system of equations implicitly assumes m distinct carrier species having m discrete mobilities, that is, no broadening of the distribution of mobilities associated with a particular carrier species is allowed.

The starting point for the QMSA procedure is to allow for the existence within the semiconductor sample of a semi-continuous mobility distribution of hole-like and electron-like species [5]. Equation (1) can thus be rewritten as

$$\sigma_{xx}(B_j) = \sum_{i=1}^{m} \frac{S_i^{xx}\Delta\mu_i}{1+\mu_i^2B_j^2} = \sum_{i=1}^{m} \frac{[s^p(\mu_i)+s^n(\mu_i)]\Delta\mu_i}{1+\mu_i^2B_j^2}$$
$$\sigma_{xy}(B_j) = \sum_{i=1}^{m} \frac{S_i^{xy}\mu_iB_j\Delta\mu_i}{1+\mu_i^2B_j^2} = \sum_{i=1}^{m} \frac{[s^p(\mu_i)-s^n(\mu_i)]\mu_iB_j\Delta\mu_i}{1+\mu_i^2B_j^2} \quad , \qquad (2)$$

where $s^n(\mu_i)$ and $s^p(\mu_i)$ are the conductivity density functions, i.e., the mobility spectra for electrons and holes, respectively, and the parameter m now defines the number of points in the final mobility spectrum rather than the number of carrier species as in Eq. (1). The QMSA uses the normalised MS envelope as an initial spectrum (first trial function) in order to solve Eq. (2) through an iterative procedure [5,6]. The resulting spectra allow the carrier concentration and mobility to be evaluated for each carrier species.

The salient features of the QMSA procedure are:

- unlike the MCF procedure, no prior assumptions need to be made about carrier number and type,
- unlike the Beck and Anderson MS, the resulting spectrum is numerically accurate,
- the QMSA procedure is fully automated and numerically stable, and
- it allows for a distribution of mobilities for each carrier type.

3. Application of QMSA to synthetic data sets

In order to verify the ability of QMSA to transform experimental Hall data into meaningful mobility spectra, synthetic data sets have been generated by substituting assumed mobility spectra into Eqs. (1) and (2). In order to simulate experimental conditions, a 1% random error is then superimposed onto the synthetic data. The maximum magnetic field is taken to be 7 T, which is typical for superconducting laboratory magnets used in Hall systems. For this value of B_{max} only carriers with mobility above 10^4/7 T = 1428 cm^2/Vs are nominally "quenched" ($\mu B = 1$), and the extraction of quantitative information about carriers with a lower mobility becomes more difficult.

In order to illustrate the ability of QMSA to reconstruct a peak-broadening effect, we first consider synthetic spectra in the form of a single gaussian peak with full-width-at-half-maximum (FWHM) $\Delta\mu/\mu$ increasing from 0.1 to 0.5, and total conductivity normalized to 1 $(\Omega\,\mathrm{cm})^{-1}$. The simulated peak is positioned at $\mu = 10^3$ cm^2/Vs, which places this example in the more challenging regime where the carriers are not fully "quenched" by the maximum magnetic field. The resulting QMSA spectra are shown in Fig. 1. Note that the shape (broadening) of the peak is reconstructed with high accuracy, even though $\mu B < 1$.

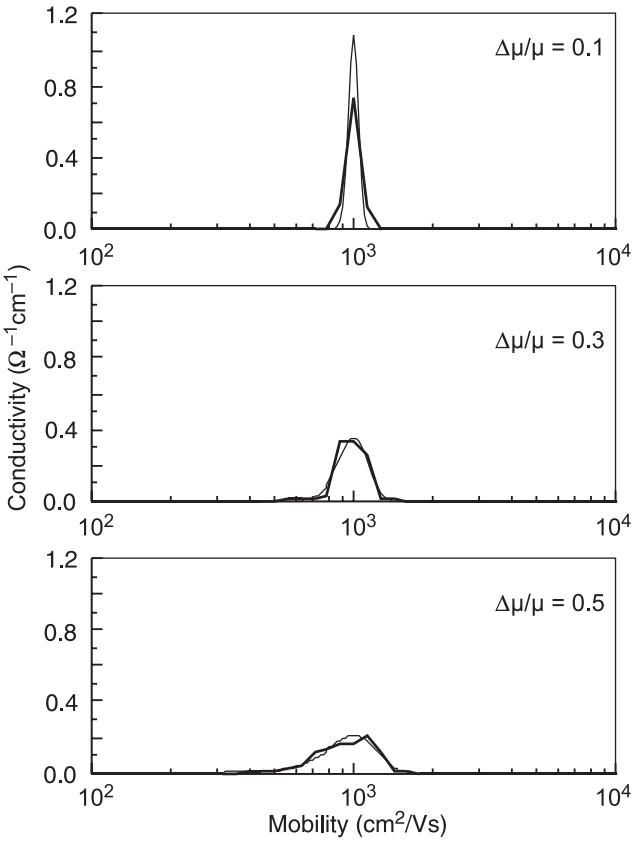

Fig. 1. Reconstruction of a single carrier peak for full width at half maximum to max. amplitude ratio ($\Delta\mu/\mu$) equal to 0.1, 0.3, and 0.5. Total conductivity is normalised to $\sigma = 1\ \Omega^{-1}\mathrm{cm}^{-1}$, centre mobility $\mu = 1000$ cm^2/Vs, and maximum magnetic field $B_{max} = 7$ T. Thin and thick lines represent original and QMSA spectra, respectively.

The issue of spectral resolution becomes especially important in cases where two distinct carriers have similar mobilities, as for example in a double layer compound-semiconductor structure with slightly different compositions. In order to test QMSA in this regard, a synthetic distribution was assumed in the form of two closely-spaced electron peaks, with mobilities $\mu_1 = 10^4$ cm^2/Vs and μ_2 variable in the range (1.5–3) $\times\ \mu_1$ (see Fig. 2). For additional realism, the distribution also contains holes with a peak mobil-

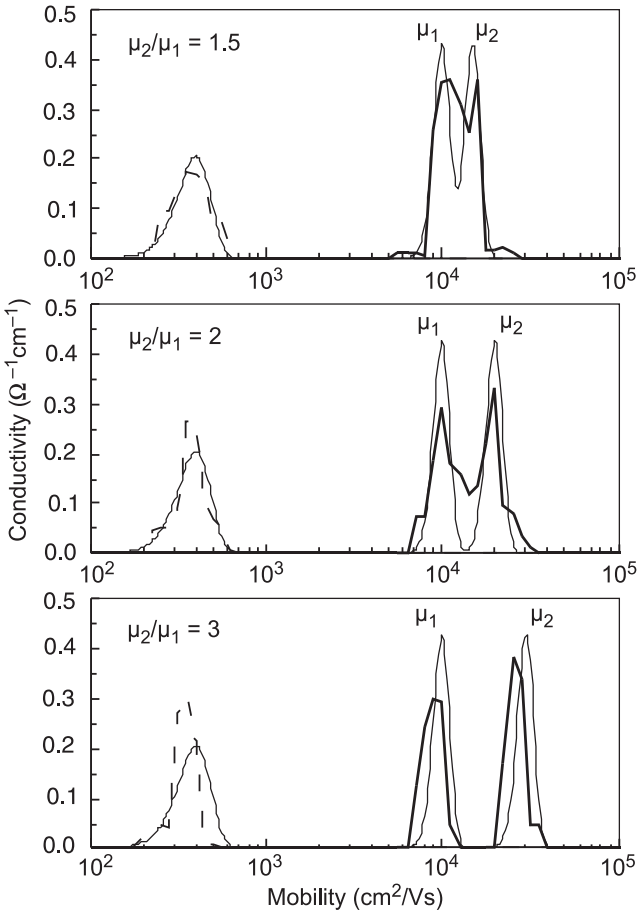

Fig. 2. Separation of two electron peaks in the high-mobility region with a low mobility hole carrier in the background, for $\mu_2/\mu_1 = 1.5$, 2, and 3. Peaks with $\mu_1 = 10^4$ cm^2/Vs represent high-mobility electrons, while the third peak with $\mu_h = 400$ cm^2/Vs corresponds to possible background holes. The total conductivity of each peak is normalised to $\sigma = 1\ \Omega^{-1}$cm^{-1}, and the maximum magnetic field is $B_{max} = 7$ T. The thin and thick lines represent original and QMSA spectra, respectively (solid-electrons and dashed-holes).

ity of 400 cm^2/Vs and $\Delta\mu/\mu = 0.5$. Such a distribution could represent, for example, an *n*-type layer (as-grown, or converted from *p*-type by ion implantation) on top of a low-mobility *p*-type layer, and with an additional surface electron with slightly lower mobility. Figure 2 shows that both electron peaks are somewhat resolved even when $\mu_2/\mu_1 = 1.5$, whereas they are fully distinct for $\mu_2/\mu_1 = 3$. The hole peak is also reliably reproduced in all three cases, despite the relation $\mu_h B_{max} << 1$.

The final synthetic example is more complicated, namely a HgCdTe multilayer structure with layering similar to that of a dual-band infrared detector operating in both the MWIR and LWIR ranges. Starting from the substrate, the assumed structure consists of the LWIR n-type layer with $x = 0.22$, the wider bandgap p-type layer with $x = 0.35$, the MWIR *n*-type layer with $x = 0.3$, and an n-type surface with CdTe passivation. Details of the structure and the densities and mobilities for each layer are given in Fig. 3. The solid thin curve is the assumed spec-

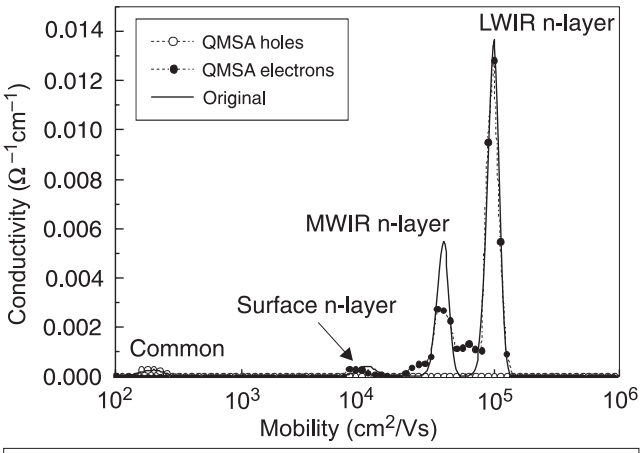

CdTe
Surface/CdTe interface: $\mu = 1\times10^4$ cm^2/Vs, $n = 1\times10^{12}$ cm^{-2}, $\mu\Delta/\mu = 0.4$
MWIR absorber: 10 μm, $x = 0.3$, $\mu = 4\times10^4$ cm^2/Vs, $n = 2\times10^{15}$ cm^{-3}, $\mu\Delta/\mu = 0.25$
Common: 4 μm, $x = 0.35$, $\mu = 200$ cm^2/Vs, $p = 1\times10^{17}$ cm^{-3}, $\mu\Delta/\mu = 0.5$
LWIR absorber: 10 μm, $x = 0.22$, $\mu = 1\times10^5$ cm^2/Vs, $n = 2\times10^{15}$ cm^{-3}, $\mu\Delta/\mu = 0.25$
Substrate

Fig. 3. Simulated and QMSA generated mobility spectrum of the two colour $Hg_{1-x}Cd_xTe$ structure.

trum, while the curves with filled and open points are the QMSA spectra for electrons and holes, respectively. We find that all of the assumed carrier species can be identified with high accuracy in the QMSA spectrum, even though the dominant contribution to the total conductivity (high mobility LWIR electrons) is 25 times greater than the smallest contribution (low mobility holes in the p-type layer). The broad background around the MWIR electron peak is a consequence of the close spacing of the LWIR and MWIR features (the mobility ratio is 2.5), and also the 1% random error superimposed on the synthetic input data.

4. QMSA of real multilayer structures

Figure 4 presents the QMSA for an AlGaAs/GaAs HEMT structure measured at room temperature and in the magnetic field range from 0.03 to 12 T. Two electron peaks are clearly resolved: one with a density of 2.1×10^{16} cm^{-3} and a mobility of 1100 cm^2/Vs corresponding to the two n^+ doped capping layers; and the other with a sheet density of 2.6×10^{11} cm^{-2} and a mobility of 7750 cm^2/Vs which corresponds to the 2D electron gas (2DEG) layer. The carrier density of the capping layers appears to be more than one order of magnitude less than the doping level specified in the MBE growth procedure which indicates that almost all the carriers have been transferred to the 2DEG residing at the $Al_{0.3}Ga_{0.7}As/GaAs$ interface. It should also be noted that the rather low value of 1100 cm^2/Vs for the capping layer electron mobility is due to the fact that it is dominated

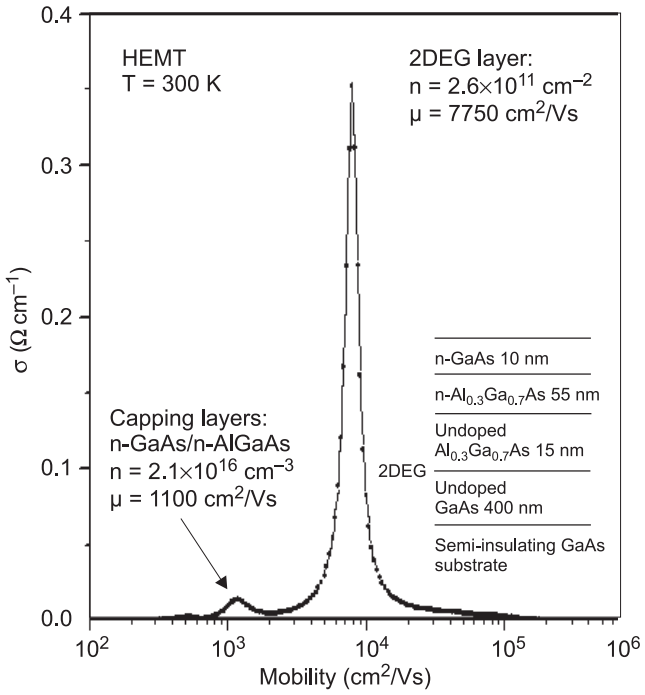

Fig. 4. Mobility spectrum of AlGaAs/GaAs HEMT structure. Contribution from 2DEG and capping layer can be identified.

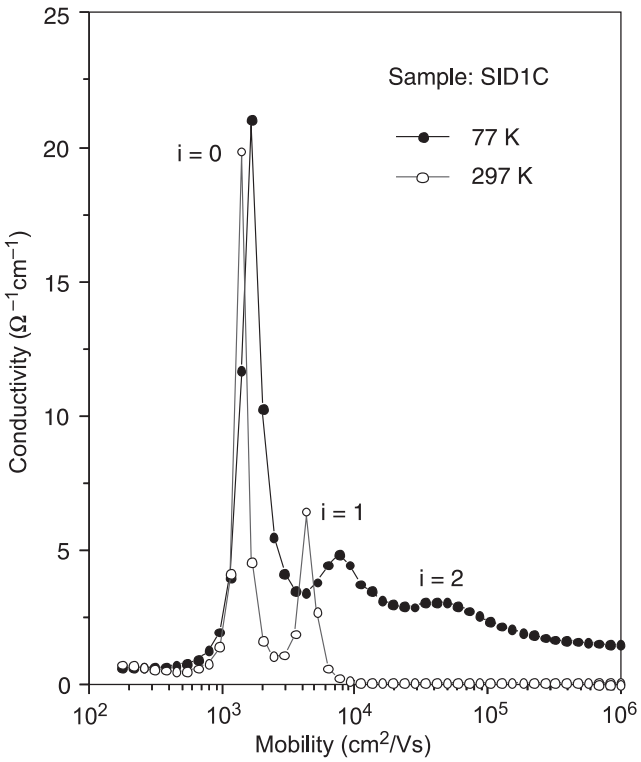

Fig. 5. Mobility spectrum of Si-δ-doped GaAs at two temperatures: 77 K and 297 K. The consecutive peaks have been identified as contributions from different quantum levels.

by the heavily doped AlGaAs layer, which is much thicker than the overlaying n^+ GaAs layer. In another example presenting QMSA ability to resolve fine details of magneto-transport, the mobility spectrum of a silicon δ-doped GaAs structure measured at two temperatures of 77 K and 297 K, respectively, is presented in Fig. 5. Peaks observed in the spectrum have been assigned to successive quantum levels with mobility increasing with the number of the level [15].

Even more detailed information can be obtained from systematic temperature analysis of mobility spectra as shown in Fig. 6. By observing shifts of peaks with changing temperature and changes in their amplitude the temperature behaviour of each individual carrier can be obtained as is shown in Fig. 7. In this case, as expected, the 2DEG density shows no temperature dependence, a feature that helps to identify this carrier species. The other carrier presents thermal activation behaviour and has been assigned to bulk GaN layer. It is important to note the QMSA sensitivity since the contribution of the GaN layer to the total conduction is only of the order of few percent.

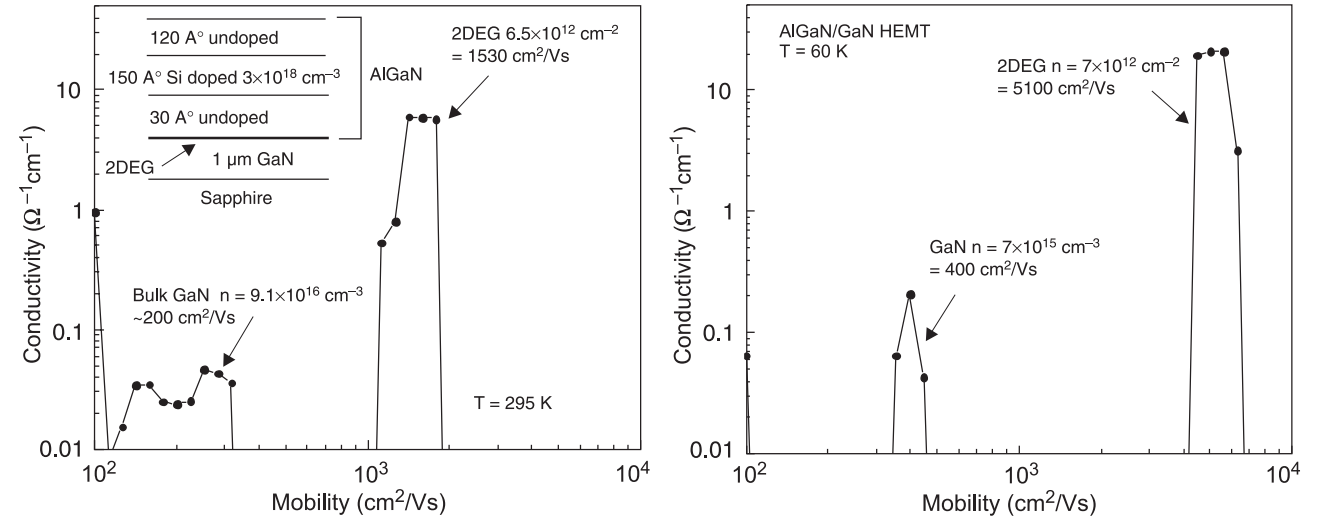

Fig. 6. QMSA of AlGaN/GaN HEMT structure at room temperature and at 60 K. Two distinct peaks are visible representing the 2DEG at the AlGaN/GaN interface and bulk GaN electrons.

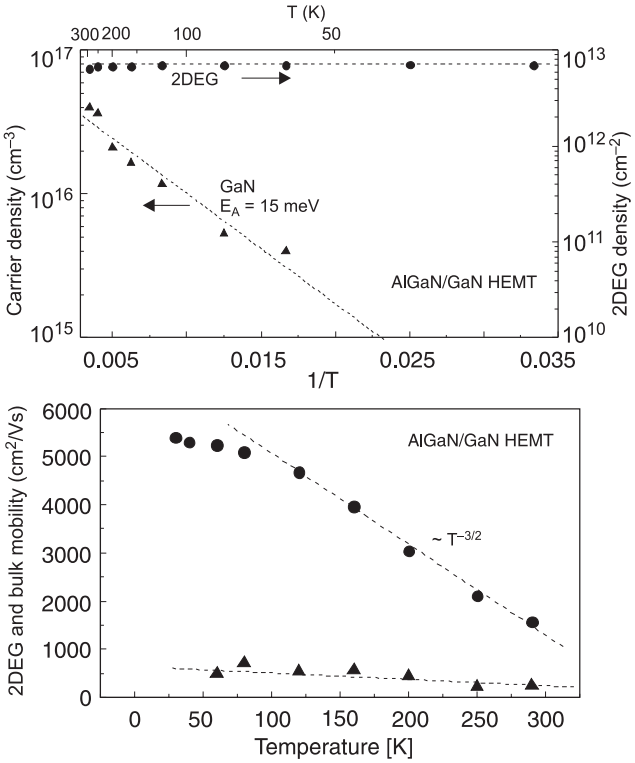

Fig. 7. Temperature dependent behaviour of carriers identified in mobility spectra of AlGaN/GaN HEMT structure from Fig. 6.

5. Conclusions

The major benefits arising from use of the QMSA procedure are that the technique is non-invasive and non-destructive to the Hall test sample, and that it will readily identify any "unexpected" carrier species which may not have been accounted for in a MCF procedure. For example, in a HEMT structure C-V electrochemical profiling is inappropriate, since the invasive nature of the technique modifies the 2DEG transport parameters as a function of etch depth. On the other hand, QMSA allows the transport parameters to be evaluated without the requirement for modifying the original device structure. As a further example, because no prior assumptions are required, mobility spectrum techniques can readily identify individual carrier species occupying discrete energy levels in quantum-confined structures. This has been demonstrated in a previous publication on delta-doped structures [15], where the individual levels have been identified. In such cases, MCF would require that the number of discrete levels at a particular temperature be known prior to attempting a fit to the Hall data. This would obviously require some form of mobility spectrum to be determined in order to decide on the number and type of carrier species to use in the fitting procedure.

In this paper, the full applicability of quantitative mobility spectrum analysis (QMSA) to multilayer structures has been shown. In particular, without any prior assumptions regarding the number and type of carriers, or their densities and mobilities, QMSA is able to identify and characterise all carriers contributing to the total sample conductivity in an automated procedure requiring no human intervention. The comparison of QMSA results with electro-chemical C-V profiling for the HBT sample indicates that QMSA has the required accuracy to be used as an industry-standard procedure. The QMSA procedure has been developed to the commercial stage, and it is readily available as stand-alone software or as part of an integrated Hall system [16].

References

1. M.C. Gold and D.A. Nelson, "Variable magnetic field Hall effect measurements and analyses of high purity Hg vacancy (p-type) HgCdTe", *J. Vac. Sci. Technol.* **A4**, 2040 (1986).
2. S.P. Tobin, G.N. Pultz, E.E. Krueger, M. Kestigian, K.K. Wong, and P.W. Norton, "Hall effect characterization of LPE HgCdTe P/n heterojunctions", *J. Electron. Mat.* **22**, 907 (1993).
3. W.A. Beck and J.R. Anderson, "Determination of electrical transport using a novel magnetic field-dependent Hall technique", *J. Appl. Phys.* **62**, 541 (1987).
4. J.R. Meyer, C.A. Hoffman, F.J. Bartoli, D.J. Arnold, S. Sivananthan, and J.P. Faurie, "Methods for magnetotransport characterization of IR detector materials", *Semicond. Sci. Technol.* **8**, 805 (1993).
5. Z. Dziuba and M. Gorska, "Analysis of the electrical conduction using an iterative method", *J. Phys. III France* **2**, 110 (1992).
6. J. Antoszewski, D.J. Seymour, L. Faraone, J.R. Meyer, and C.A. Hoffman, "Magneto-transport characterization using quantitative mobility spectrum analysis", *J. Electron. Mater.* **24**, 1255 (1995).
7. J.R. Meyer, C.A. Hoffman, F.J. Bartoli, J. Antoszewski, L. Faraone, S.P. Tobin, P.W. Norton, C.K. Ard, D.J. Reese, L. Colombo, and P.K. Liao, "Advanced magneto-transport characterisation of LPE-grown HgCdTe by QMSA", *J. Electron. Mater.* **25**, 1157 (1996).
8. J.R. Meyer, C.A. Hoffman, J. Antoszewski, and L. Faraone, "Quantitative mobility spectrum analysis of multicarrier conduction in semiconductors", *J. Appl. Phys.* **81**, 709 (1997).
9. J. Antoszewski, J.M. Dell, L. Faraone, L.S. Tan, A. Raman, S.J. Chua, D.S. Holmes, J.R. Lindemuth, and J.R. Meyer, "Evaluation of III-V multilayer transport parameters using QMSA", *Mat. Sci. Eng.* **B44**, 65 (1997).
10. J.R. Meyer, C.A. Hoffman, F.J. Bartoli, J. Antoszewski, and L. Faraone, "Mobility spectrum analysis for magnetic-field-dependent Hall and resistivity data", *US Patent* Nr. 5,789,931 (1998).
11. I. Vurgaftman, J.R. Meyer, C.A. Hoffman, D. Redfern, J. Antoszewski, L. Faraone, and J.R. Lindemuth, "Improved quantitative mobility spectrum analysis for Hall characterization", *J. Appl. Phys.* **84**, 4966 (1998).
12. I. Vurgaftman, J.R. Meyer, C.A. Hoffman, S. Cho, J.B. Ketterson, L. Faraone, J. Antoszewski, and J.R. Lindemuth, "Quantitative mobility spectrum analysis (QMSA) for Hall

characterization of electrons and holes in anisotropic bands", *J. Electron. Mater.* **28**, 548 (1999).
13. J.R. Meyer, I. Vurgaftman, D.A. Redfern, J. Antoszewski, L. Faraone, and J.R. Lindemuth, "Improved quantitative mobility spectrum analysis of magnetic-field-dependent Hall and resistivity data", *US Patent* Nr. 6,100,704 (2000), US Patent Nr. 6,100,704 (2000).
14. J. Antoszewski, D. Redfern, L. Faraone, J. R. Meyer, I. Vurgaftman, and J. Lindemuth, "Comment on mobility spectrum computational analysis using a maximum entropy approach", *Phys. Rev.* **E69**, 038701 (2004).
15. G. Li, J. Antoszewski, W. Xu, N. Hauser, and C. Jagadish, "Study of subband electronic structure of Si δ-doped GaAs using magnetotransport measurements in tilted magnetic fields", *J. Appl. Phys.* **79**, 8482 (1996).
16. Lakeshore Crotronics Ltd., www.lakeshore.com.

